

# SEPARATING THE CONJOINED RED CLUMP IN THE GALACTIC BULGE: KINEMATICS AND ABUNDANCES

ROBERTO DE PROPRIIS<sup>1</sup>, R. MICHAEL RICH<sup>2</sup>, ANDREA KUNDER<sup>1</sup>, CHRISTIAN I. JOHNSON<sup>2,8</sup>, ANDREAS KOCH<sup>3</sup>, SARAH BROUGH<sup>4</sup>, CHRISTOPHER J. CONSELICE<sup>5</sup>, MADUSHA GUNAWARDHANA<sup>6</sup>, DAVID PALAMARA<sup>7</sup>, KEVIN PIMBLETT<sup>7</sup>, AND DINUKA WIJESINGHE<sup>6</sup>

<sup>1</sup> Cerro Tololo Inter-American Observatory, La Serena, Chile

<sup>2</sup> Department of Physics and Astronomy, University of California, Los Angeles, CA, USA

<sup>3</sup> Department of Physics and Astronomy, University of Leicester, University Road, Leicester LE1 7RH, UK

<sup>4</sup> Australian Astronomical Observatory, Epping, NSW, Australia

<sup>5</sup> Department of Physics and Astronomy, University of Nottingham, Nottingham NG7 2RD, UK

<sup>6</sup> Sydney Institute of Astronomy, School of Physics A29, University of Sydney, NSW, Australia

<sup>7</sup> School of Physics, Monash University, Clayton, VIC, Australia

Received 2011 January 22; accepted 2011 April 1; published 2011 April 25

## ABSTRACT

We have used the AAOMEGA spectrograph to obtain  $R \sim 1500$  spectra of 714 stars that are members of two red clumps in the Plaut Window Galactic bulge field ( $l, b = (0^\circ, -8^\circ)$ ). We discern no difference between the clump populations based on radial velocities or abundances measured from the  $Mgb$  index. The velocity dispersion has a strong trend with  $Mgb$ -index metallicity, in the sense of a declining velocity dispersion at higher metallicity. We also find a strong trend in mean radial velocity with abundance. Our red clump sample shows distinctly different kinematics for stars with  $[Fe/H] < -1$ , which may plausibly be attributable to a minority classical bulge or inner halo population. The transition between the two groups is smooth. The chemo-dynamical properties of our sample are reminiscent of those of the Milky Way globular cluster system. If correct, this argues for no bulge/halo dichotomy and a relatively rapid star formation history. Large surveys of the composition and kinematics of the bulge clump and red giant branch are needed to further define these trends.

**Key words:** Galaxy: bulge – Galaxy: formation – Galaxy: halo

*Online-only material:* color figures

## 1. INTRODUCTION

The existence of a prominent bar in the Galactic bulge is now well established from multiple lines of evidence (e.g., Liszt & Burton 1980; Blitz & Spergel 1991; Stanek et al. 1994; Babusiaux & Gilmore 1995). The large-scale kinematics of the bulge sampled by the BRAVA (Bulge Radial Velocity Assay) survey (Rich et al. 2007; Howard et al. 2008, 2009) can be fitted with simple cylindrical rotation and little or no classical spheroidal component (Shen et al. 2010), a conclusion also reached (albeit at lower confidence) from proper-motion surveys (Rattenbury et al. 2007). Our “bulge” appears to consist of a peanut-shaped bar, reminiscent of the “pseudobulges” defined by Kormendy & Kennicutt (2004) and encountered elsewhere (Kormendy & Barentine 2010).

At the same time, this result is puzzling. The BRAVA data imply that our Galaxy has not undergone any significant merger since the epoch at which the disk formed, in contrast with expectations from simulations within  $\Lambda$ CDM cosmological models (e.g., Bullock & Johnston 2005; Cooper et al. 2010). However, it is well known that stars in the bulge are metal-rich and  $\alpha$ -enhanced, indicating a rapid star formation history typical of classical bulges (McWilliam & Rich 1994; Ballero et al. 2007). The observation of an abundance gradient for bulge stars (Zoccali et al. 2008) and a correlation between abundance and kinematics (Babusiaux et al. 2010) may also indicate the presence of a classical spheroidal component, although dynamical data (Shen et al. 2010) seem to be inconsistent with this. On the other hand, detailed abundances for subgiants and lensed dwarfs are more similar to those of the thick disk, in

accordance with a pseudobulge formation scenario (Melendez et al. 2008; Alves-Brito et al. 2010; Bensby et al. 2010; Ryde et al. 2010).

Adding to the complexity, the red clump in the bulge color-magnitude diagram appears doubled at  $|l| > 5^\circ$  (McWilliam & Zoccali 2010; Nataf et al. 2010). McWilliam & Zoccali (2010) carry out a very careful analysis of the photometric properties of the double red clump and conclude that the splitting of the red clump is due to a distance effect and that the bulge may contain an X-shaped structure, extending from the ends of the bar. So far, the only spectroscopic study of this population has been carried out by Rangwala et al. (2009) using Fabry–Perot imaging spectroscopy in Baade’s Window and some adjacent fields, and their results suggest that there is a metallicity gradient with galactic latitude (Rangwala & Williams 2009), as well as dynamical differences, which would be more consistent with the presence of a stream, although it is clear that more accurate kinematics and metallicities are needed to truly understand the nature of this feature.

Here we present the first low-resolution survey of a field at  $l = 0^\circ$  and  $b = -8^\circ$  (Plaut’s Window) specifically targeting the red clump stars. We analyze the kinematics and metallicity of stars belonging to each peak and derive the metallicity-kinematics trends. Although this is clearly a “first look” exploratory analysis, our data imply that the two populations are dynamically and chemically similar and favor the X-shaped bulge hypothesis proposed by McWilliam & Zoccali (2010).

## 2. DATA REDUCTION AND ANALYSIS

The data for this project were kindly provided by the Galaxy and Mass Assembly Survey (GAMA; Driver et al. 2010). This survey is observing three  $12 \text{ deg}^2$  fields at  $9^h$ ,  $12^h$ , and  $15^h$

<sup>8</sup> National Science Foundation Astronomy and Astrophysics Postdoctoral Fellow

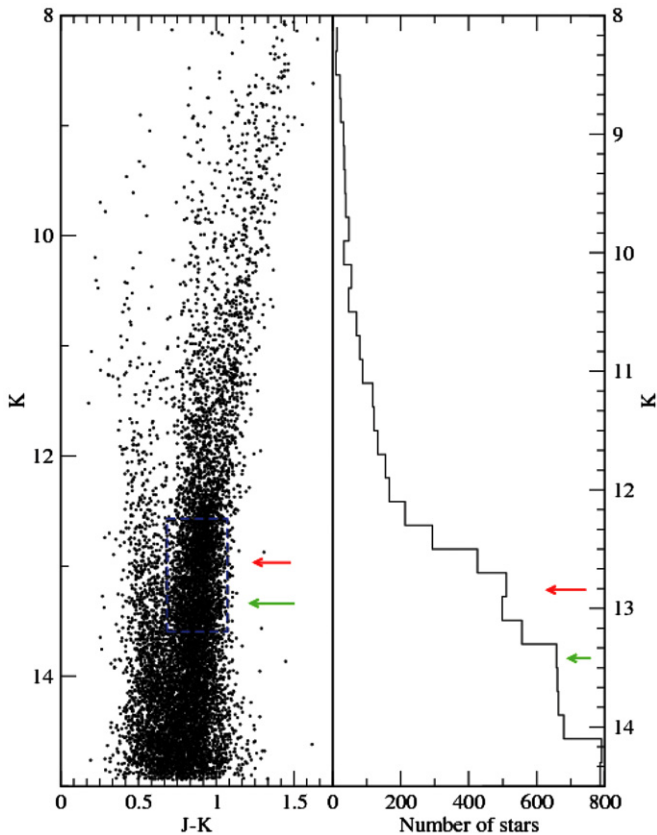


**Figure 1.** Color-magnitude diagram (from 2MASS data) for our bulge field is shown in the left-hand panel of this figure. The blue box shows the (non-dereddened) selection limits used. The right-hand panel shows the histogram of the distribution of stars in  $K_0$  and the two peaks identified by the GMM algorithm, marked by arrows (red for the brighter peak and green for the fainter peak).

(A color version of this figure is available in the online journal.)

R.A. using the AAΩ multifiber spectrograph on the Anglo-Australian Telescope (AAT). At the end of 2010 May, it was found to be impossible to reach either GAMA field during the last two hours of the night, at sufficiently low airmass. The survey kindly offered to observe one of the fields containing a double red clump for us.

Two 400-fiber configurations were observed for Plaut’s Window (where the two red clumps are relatively well separated and the extinction is lower). The target stars were selected from the Two Micron All Sky Survey (2MASS; Skrutskie et al. 2006), in a  $2^\circ$  (diameter) field. Bulge stars were required to have  $K_0 = 7.5(J - K)_0 + 9$  to exclude disk contamination and to lie between  $12.5 < K_0 < 13.5$  and  $0.58 < (J - K)_0 < 1.00$  to probe the double red clump. Magnitudes were dereddened from the Schlegel et al. (1998) maps. Figure 1 shows the color-magnitude diagram of the target stars. The two red clumps are identified by applying a Gaussian Mixture Modeling (GMM) algorithm to the data (Muratov & Gnedin 2010), which also assigns to each star a probability of belonging to either peak. The magnitudes of the two red clump peaks are in good agreement with those reported by McWilliam & Zoccali (2010) for this region. By necessity, we used the same spectroscopic setup as employed for the GAMA survey; this covers the entire optical window, from about 3700 to 9000 Å at a resolution of about 1500. Although this is somewhat less than optimal for deter-

mining stellar radial velocities and abundances, it suffices for our initial analysis of this field.

The data were reduced using the automated pipeline supplied by AAΩ. A total of 714 stars were eventually observed. The typical signal-to-noise ratios of these spectra are about 10 at Ca H&K, 20 in the Mgb region, and 50 for the calcium triplet wavelength range. Radial velocities were measured by cross-correlation against stellar templates using the runz program (Saunders et al. 2004) which is specifically written for analysis of AAΩ data. Among the several templates available in runz we imposed the choice of a K-giant template, if this was not automatically selected by the program. Of the 714 targets, 631 returned a valid radial velocity ( $>95\%$  probability that the measured velocity is correct from the height of the correlation peak). Typical velocity errors are  $1/10$  of a resolution element, or  $25 \text{ km s}^{-1}$  for the  $R \sim 1500$  of GAMA data, but no stars with a velocity error above  $2\sigma$  ( $50 \text{ km s}^{-1}$ ) were used for our analysis.

We experimented with a number of techniques to measure metal abundances, including the non-SEGUE stellar parameters pipeline (e.g., Li et al. 2010 and references therein) and the calcium triplet (although red clump giants were outside the luminosity range of the calibrations). We eventually found that the most reliable measurements (when compared with the high-resolution abundances measured for giants in Plaut’s Window by Johnson et al. 2011) were given by using the Mgb Lick index (Worthey 1994; Ibata & Gilmore 1995). We measured this index and its errors (based on the CCD noise parameters and the radial velocity errors) using the LECTOR software.<sup>9</sup> The typical error in measuring the Mgb index is about 5%.

In order to derive metal abundances from the Mgb index, we used fitting functions for cool stars by Worthey et al. (1994). We assumed  $\log g = 2.25$  which is appropriate for red clump giants based on the Padova isochrones (Marigo et al. 2008). Temperatures were estimated from the dereddened  $J - K$  color, using the  $T_{\text{eff}}$ —color relations by Houdashelt et al. (2000). This approach was used by Cote et al. (1999), among others, to measure the abundance of red giants in M31, although we found that only Mgb can be reliably measured in our data. We derived metallicities for 545 stars in our data.

The typical random error in metal abundance is  $\pm 0.1$  dex, based on the error in the index measurement, but of course there are systematic errors depending on the assumed values of  $\log g$  and  $T_{\text{eff}}$ . Altering  $\log g$  by 0.1 at the same temperature yields a change in  $[\text{Fe}/\text{H}]$  of around 0.15 dex, while altering  $T_{\text{eff}}$  by 100 K yields abundance changes of 0.3 dex. In addition, our data are not on the Lick system as no standards were observed, and this may introduce a systematic effect of the order of 0.2 dex in the measurement of metal abundances. We used some Lick standards observed by ELODIE (Moultaka et al. 2004) to measure Mgb and find that our abundances tend to be  $\sim 0.2$  dex too low, which would bring our data in better agreement with high-resolution measurements by Johnson et al. (2011). In addition, the known  $\alpha$  enhancement of the bulge (e.g., McWilliam & Rich 1994) means that the Mgb abundance may overestimate the actual  $[\text{Fe}/\text{H}]$  of the stars, although it is probably a better proxy of the total metal abundance.

### 3. THE NATURE OF THE RED CLUMP

Figure 2 shows the radial velocity distribution for red clump stars derived from our data. The mean heliocentric radial

<sup>9</sup> [http://www.iac.es/galeria/vazdekis/vazdekis\\_software.html](http://www.iac.es/galeria/vazdekis/vazdekis_software.html)

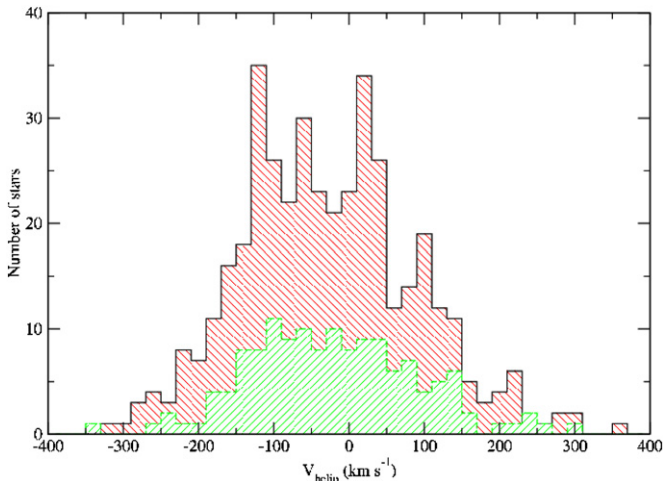


**Figure 2.** Radial velocity distribution of stars belonging to each red clump peak (red for the brighter peak and green for the fainter peak as in Figure 1). (A color version of this figure is available in the online journal.)

velocity for the entire sample is  $-15 \pm 5 \text{ km s}^{-1}$  (rms), which is equivalent to a velocity of  $-4 \text{ km s}^{-1}$  (Galactocentric standard of rest), consistent with data from the BRAVA survey. The radial velocity dispersion is  $110 \pm 5 \text{ km s}^{-1}$ , which is somewhat larger than what is measured for this galactic latitude by BRAVA, although we are looking at a fainter sample. The intrinsic dispersion and its error were computed following Spaenhauer et al. (1992). The higher velocity dispersion seems to be due to a low metallicity population that may not be present in the BRAVA data.

Stars in the first (brighter) peak have a mean heliocentric velocity of  $-18 \pm 6 \text{ km s}^{-1}$  and velocity dispersion of  $109 \pm 5 \text{ km s}^{-1}$ , while stars belonging to the second (fainter) red clump have mean velocity of  $-6 \pm 8 \text{ km s}^{-1}$  and velocity dispersion of  $113 \pm 9 \text{ km s}^{-1}$ . Within the errors, stars in both red clumps have the same mean velocity and velocity dispersion and therefore appear to have the same kinematics. This would appear to be at odds with claims for a difference in the kinematics of the two red clumps (Rangwala et al. 2009), although more sightlines are needed. Application of the GMM algorithm shows that there is  $<50\%$  chance that the velocity distribution is bimodal. A Kolmogorov–Smirnov (K-S) two-sample test yields an 88% chance that the two distributions come from the same parent. The  $t$ -test and  $F$ -test show that the two distributions do not have significantly different means or variances.

Figure 3 shows the distribution in metal abundance for stars in both clumps. The distribution for all stars has a mean  $[\text{Fe}/\text{H}]$  of  $-0.61 \pm 0.03$ . The distribution is consistent with that observed for red giants in Baade’s Window by McWilliam & Rich (1994), the high-resolution metallicities in Plaut’s Window (overplotted in the figure) measured by Johnson et al. (2011), and the expectations from the metallicity gradient measured by Zoccali et al. (2008), but with a systematic offset ( $\sim 0.2$  dex) probably due to the lack of an absolute calibration based on Lick standards.

Stars in the first peak have mean  $[\text{Fe}/\text{H}]$  of  $-0.55 \pm 0.03$  with a dispersion of 0.58, while stars in the second peak have mean  $[\text{Fe}/\text{H}]$  of  $-0.67 \pm 0.03$  with a dispersion of 0.62. Again, the GMM algorithm returns a distribution consistent with a unimodal distribution. Within the errors, stars belonging to each red clump have the same  $[\text{Fe}/\text{H}]$  abundances. The K-S test gives a 73% probability for the two clumps to be drawn from the

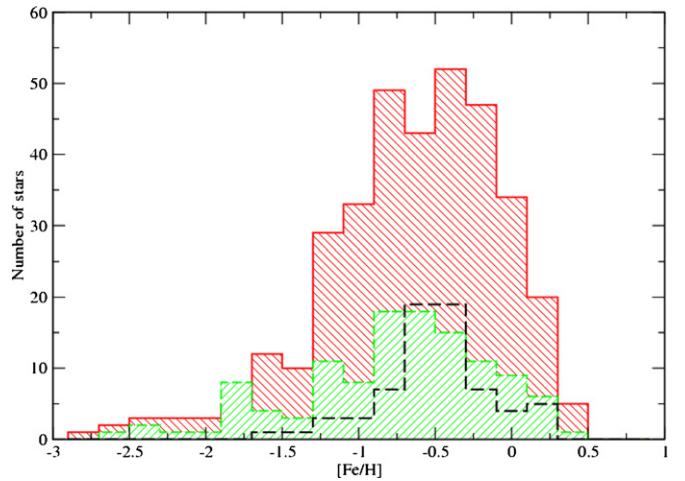


**Figure 3.**  $[\text{Fe}/\text{H}]$  distribution of stars belonging to each red clump peak (red for the brighter peak and green for the fainter peak as in Figure 2). The black dashed histogram shows the distribution of metal abundances for red giants studied by Johnson et al. (2011).

(A color version of this figure is available in the online journal.)

same distribution. Similarly, the  $t$ -test and  $F$ -test show that two samples do not have significantly different means or variances.

One aim in this work is to compare the kinematics and metallicities of stars belonging to the two red clumps identified in the galactic bulge by McWilliam & Zoccali (2010) and Nataf et al. (2010). Our data show that the two populations have the same kinematics and metal abundance, which suggests that the difference in luminosity between the two red clumps is a distance effect. In other words, the two red clumps are observed at the two ends of the  $\sim 2$  kpc bar that constitutes the bulge of the Milky Way. These data are therefore consistent with the analysis by McWilliam & Zoccali (2010), attributing the double red clump to the existence of X-shaped protrusions at the end of the Milky Way bar (i.e., an X-shaped bulge). If these stars lie at the end of a bar, then the metal abundance gradient across the structure is expected to be quite small.

An alternate possibility is that the two red clumps are different in helium content. Helium abundance variations are believed to exist (from indirect evidence) in massive globular clusters in our Galaxy (e.g., Carretta et al. 2009). Helium enhancement would produce differences in the luminosity of the red clump stars (D’Antona et al. 2010), but any process capable of producing the necessary helium enhancement would also overproduce metals. We would presume that populations with different chemical abundances might also have different kinematics.

#### 4. ABUNDANCE TRENDS WITH KINEMATICS

Classical bulges present a number of abundance trends with kinematics, some of which are also observed in the Galactic bulge. Zoccali et al. (2008) have measured a metallicity gradient with radius. Babusiaux et al. (2010) find a trend between metal abundance and velocity dispersion in Baade’s Window and two lower ( $b = -6^\circ$  and  $-8^\circ$ ) galactic latitude fields, arguing for a two-component bulge, with a metal-rich system comprising the bar and a metal-poor spheroid or thick disk, the relative contribution from each of these varying with galactic latitude.

We plot the mean velocity (upper panel) and velocity dispersion (lower panel) as a function of metallicity in Figure 4. We plot all stars (black points), stars in the first (brighter) peak (red points), and stars in the second (fainter) peak (green points)



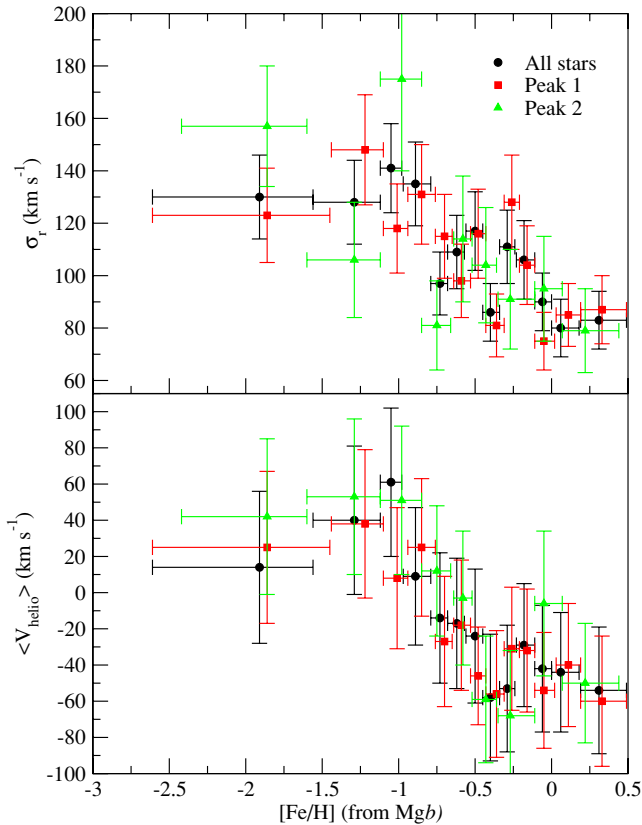


**Figure 4.** Dependence of heliocentric mean velocity on metallicity (lower panel) and radial velocity dispersion (upper panel) for stars in our field. See legend in the figure to identify the samples. The bins are chosen to contain the same number of stars, sorted by metal abundance; the horizontal error bars represent the range of metallicities in each bin. The vertical error bars are the errors on mean radial velocity and velocity dispersion, as appropriate.

(A color version of this figure is available in the online journal.)

separately. Stars in each group are binned in bins containing the same number of stars after sorting by metal abundance. For each of the groups we consider (all stars in the brighter and fainter peaks) the bins span a non-overlapping range in metal abundance. Stars in both red clumps appear to obey the same relations between metallicity and kinematics. This confirms that the two populations do not differ in kinematic properties or abundances, which is more consistent with a projection effect and an X-shaped bulge structure.

The data shown in Figure 4 show a clear trend for increasing velocity dispersion with decreasing metal abundance. This is similar to what is found by Johnson et al. (2011) in their higher resolution data. Babusiaux et al. (2010) use two fields at  $b = -6^\circ$  and  $b = -12^\circ$  and although there are few stars at  $[\text{Fe}/\text{H}] < -1$  in their data, there is a hint of an increase in the velocity dispersion at lower metal abundances, in agreement with our observations. Vieira et al. (2007) find a flat distribution of metallicity with velocity dispersion (from proper-motion data) for stars with  $[\text{Fe}/\text{H}] > -1$ , which is not in disagreement with our observations, where most of the increase in velocity dispersion takes place for lower metallicity stars.

For stars with  $[\text{Fe}/\text{H}] > -1$  the velocity dispersion is in good agreement with that measured for BRAVA M giants and does not depend strongly on metal abundance, which is broad agreement with what measured by Vieira et al. (2007) in Plaut’s Window and the two lower galactic latitude fields in Babusiaux et al. (2010). However, at  $[\text{Fe}/\text{H}] < -1$  there appears to be a (at

face value) smooth transition to a dynamically hot component. Similarly, in the upper panel of Figure 4 we see that the metal-rich component appears to have significant mean heliocentric velocity, while at  $[\text{Fe}/\text{H}] < -1$  one observes a smooth trend toward a relatively static velocity component. One caveat in this is that the metallicity errors are large, and we cannot rule out a bimodal distribution with the “wings” of the errors simulating a smoother transition between the two behaviors, although this would require a correlation between metallicity errors, measured radial velocity, and velocity dispersion.

The metal-rich stars are best interpreted as part of the bar/bulge structure. Their kinematics show evidence of rotational support and bulk rotation and are consistent with data from the BRAVA survey in this region. The behavior of the more metal-poor component, showing high velocity dispersion, and low to zero velocity relative to the Sun may be explained by a classical bulge or by inner halo stars. With a mean metal abundance of  $[\text{Fe}/\text{H}] \sim -1.5$  these stars appear to be best interpreted (at least provisionally) as an inner halo population, although bulges can of course be metal poor as well. This is consistent with the observations by Zoccali et al. (2008) and Babusiaux et al. (2010), albeit for a single sightline. However, the BRAVA data show no classical bulge component fitting their dynamical model (Shen et al. 2010). One possibility is that by selecting M giants and using the calcium triplet as their main radial velocity indicator, BRAVA may be biased against lower metallicity stars and therefore preferentially miss the high  $\sigma$  component.

The properties of galactic globular clusters present an interesting analogy with what is observed here: metal-rich clusters, with mean  $[\text{Fe}/\text{H}]$  of  $\sim -0.7$ , are believed to be associated with the bulge and are supported at least in part by rotation, whereas inner halo clusters have mean  $[\text{Fe}/\text{H}]$  of  $\sim -1.6$ , their kinematics are dominated by random motions and at most very slow rotation. It is tempting to speculate that the two components we see in our data are analogous to the metal-poor and metal-rich globular clusters, whose properties they appear to share to some extent (cf. Babusiaux et al. 2010 for a similar two-component model for the bulge). Ortolani et al. (1995), Zoccali et al. (2003), and Clarkson et al. (2008) have argued, on the basis of isochrone fits to bulge globular clusters and field stars, that the bulge formed nearly coevally with the halo. Most globular clusters in the inner halo formed within  $\pm 1$  Gyr of each other (Marin-Franch et al. 2009). If this applies to bulge stars as well, it would imply a rapid star formation process, at least for the inner regions ( $< 20$  kpc) of the Milky Way.

If this is the case, the smooth transition between the metal-rich and metal-poor subsystems, with a “turnover” point at  $[\text{Fe}/\text{H}] \sim -1$ , may imply that the bulge and halo components are continuous and that there is no clear dichotomy between the two (modulo the large errors in metal abundance). This would be consistent with the BRAVA result that the bulge was formed (in a dynamical sense) from secular evolution at high redshift. As long as the stars also formed rapidly, the observed  $\alpha$ -element enhancements are not in disagreement with this hypothesis.

This publication makes use of data products from the Two Micron All Sky Survey, which is a joint project of the University of Massachusetts and the Infrared Processing and Analysis Center/California Institute of Technology, funded by the National Aeronautics and Space Administration and the National Science Foundation. This material is based upon work supported by the National Science Foundation under award No. AST-1003201 to C.J. R.M.R. acknowledges support from

grant AST 0709479 from the National Science Foundation. We thank the GAMA survey for allowing us to use two hours of AAT time to carry out this program. We would also like to thank Scott Croom, David Wilkerson, Rob Sharp, and Will Sutherland.

*Facility:* AAT (2dF)

## REFERENCES

- Alves-Brito, A., Melendez, J., Asplund, M., Ramirez, I., & Yong, D. 2010, *A&A*, **513**, 35
- Babusiaux, C., & Gilmore, G. 1995, *MNRAS*, **358**, 1309
- Babusiaux, C., et al. 2010, *A&A*, **519**, 77
- Ballero, S. K., Matteucci, F., Origlia, R., & Rich, R. M. 2007, *A&A*, **467**, 123
- Bensby, T., et al. 2010, *A&A*, **521**, L57
- Blitz, L., & Spergel, D. N. 1991, *ApJ*, **379**, 631
- Bullock, J. S., & Johnston, K. V. 2005, *ApJ*, **635**, 931
- Carretta, E., et al. 2009, *A&A*, **505**, 117
- Clarkson, W., et al. 2008, *ApJ*, **684**, 1110
- Cooper, A. P., et al. 2010, *MNRAS*, **406**, 744
- Cote, P., Oke, J. B., & Cohen, J. G. 1999, *AJ*, **118**, 1645
- D’Antona, F., Ventura, P., Caloi, V., D’Ercole, A., Vesperini, E., Carini, R., & Di Criscienzo, M. 2010, *ApJ*, **715**, L63
- Driver, S. P., et al. 2010, arXiv:1009.0614
- Houdashelt, M. L., Bell, R. A., & Sweigart, A. V. 2000, *AJ*, **119**, 1448
- Howard, C. D., Rich, R. M., Reitzel, D. B., Koch, A., De Propriis, R., & Zhao, H.-S. 2008, *ApJ*, **688**, 1060
- Howard, C. D., et al. 2009, *ApJ*, **702**, L153
- Ibata, R. A., & Gilmore, G. 1995, *MNRAS*, **275**, 605
- Johnson, C. I., Rich, R. M., Fulbright, J. P., Valenti, A., & McWilliam, A. 2011, arXiv:1103.2143
- Kormendy, J., & Barentine, J. C. 2010, *ApJ*, **715**, L176
- Kormendy, J., & Kennicutt, R. 2004, *ARA&A*, **42**, 603
- Li, H. N., et al. 2010, *A&A*, **521**, 10
- Liszt, H. S., & Burton, W. B. 1980, *ApJ*, **236**, 779
- Marigo, P., Girardi, L., Bressan, A., Groenewegen, M. A. T., Silva, L., & Granato, G. L. 2008, *A&A*, **482**, 883
- Marin-Franch, A., et al. 2009, *ApJ*, **694**, 1498
- McWilliam, A., & Rich, R. M. 1994, *ApJS*, **91**, 749
- McWilliam, A., & Zoccali, M. 2010, *ApJ*, **724**, 1491
- Melendez, J., et al. 2008, *A&A*, **484**, L21
- Moultaka, J., Ilievsky, S. A., Prugniel, P., & Soubiran, C. 2004, *PASP*, **116**, 693
- Muratov, A. L., & Gnedin, O. Y. 2010, *ApJ*, **718**, 1266
- Nataf, D. M., Udalski, A., Gould, A., Fouqué, P., & Stanek, K. Z. 2010, *ApJ*, **721**, L28
- Ortolani, S., Renzini, A., Gilmozzi, R., Marconi, G., Barbuy, B., Bica, E., & Rich, R. M. 1995, *Nature*, **377**, 701
- Rangwala, N., & Williams, T. B. 2009, *ApJ*, **702**, 414
- Rangwala, N., Williams, T. B., & Stanek, K. Z. 2009, *ApJ*, **691**, 1387
- Rattenbury, N. J., Mao, S., Sumi, T., & Smith, M. C. 2007, *MNRAS*, **378**, 1064
- Rich, R. M., Reitzel, D. B., Zhao, H. S., & Howard, C. D. 2007, *ApJ*, **658**, L29
- Ryde, N., et al. 2010, *A&A*, **509**, 20
- Saunders, W., Cannon, R., & Sutherland, W. 2004, AAO Newslett., **106**, 16
- Schlegel, D. J., Finkbeiner, D. B., & Davis, M. 1998, *ApJ*, **500**, 525
- Shen, J., Rich, R. M., Kormendy, J., Howard, C. D., De Propriis, R., & Kunder, A. 2010, *ApJ*, **720**, L72
- Skrutskie, M. F., et al. 2006, *AJ*, **131**, 1163
- Spaenhauer, A., Jones, B. F., & Whitford, A. E. 1992, *AJ*, **103**, 297
- Stanek, K. Z., Mateo, M., Udalski, A., Szymanski, M., Kaluzny, J., & Kubiak, M. 1994, *ApJ*, **429**, L73
- Vieira, K., et al. 2007, *AJ*, **134**, 1432
- Worthey, G. 1994, *ApJS*, **95**, 107
- Worthey, G., Faber, S. M., Gonzalez, J. J., & Burstein, D. 1994, *ApJS*, **94**, 687
- Zoccali, M., Hill, V., Lecureur, A., Barbuy, B., Renzini, A., Minniti, D., Gómez, A., & Ortolani, S. 2008, *A&A*, **486**, 177
- Zoccali, M., et al. 2003, *A&A*, **399**, 931